

Initial proposal of a smart cement-based material to enhance the service-life of reinforcement concrete structures

Original

Initial proposal of a smart cement-based material to enhance the service-life of reinforcement concrete structures / Martínez-Ibernón, Ana; Antonaci, Paola; Anglani, Giovanni. - In: MATEC WEB OF CONFERENCES. - ISSN 2261-236X. - ELETTRONICO. - 378:(2023), pp. 1-6. (Intervento presentato al convegno SMARTINCS'23 Conference on Self-Healing, Multifunctional and Advanced Repair Technologies in Cementitious Systems tenutosi a Ghent, Belgium nel May 22-23, 2023) [10.1051/matecconf/202337805003].

Availability:

This version is available at: 11583/2983307 since: 2023-10-25T08:11:36Z

Publisher:

EDP Sciences

Published

DOI:10.1051/matecconf/202337805003

Terms of use:

This article is made available under terms and conditions as specified in the corresponding bibliographic description in the repository

Publisher copyright

(Article begins on next page)

Initial proposal of a smart cement-based material to enhance the service-life of reinforcement concrete structures

Ana Martínez-Ibernón¹; Paola Antonaci², Giovanni Anglani²

¹IDM - Instituto Interuniversitario de Reconocimiento Molecular y Desarrollo Tecnológico, Universitat Politècnica de València, Camino de Vera s/n, Valencia;

²Politecnico di Torino, Department of Structural, Geotechnical and Building Engineering, Corso Duca degli Abruzzi 24, Turin 10129, Italy

Abstract. The sustainable development of societies can be pursued by simultaneously avoiding the depletion of materials and resources and reducing the greenhouse gases emissions, with related climatic change effects. In order to get this, the extension of structures service-life plays a significant role in saving natural resources, decreasing the overall anthropogenic carbon-footprint, and reducing building and demolition wastes. In order to achieve such prolongation of structures service-life, one of the most promising approaches is the development of Smart Structures. These are defined as structures that are able to self-sense some external stimuli such as stress or temperature variations, and internal conditions such as chloride penetration, concrete carbonatation, etc. Consequently, ongoing damage phenomena can be detected promptly, thus allowing to implement suitable countermeasures in the most efficient way. Smart Structures can also process the information and respond autonomously in real time by using smart materials technologies such as self-healing technology. In this study we propose a preliminary version of a smart material system with self-healing and sensing properties, to demonstrate its effectiveness at a proof of concept level. The effectiveness of an active, capsule-based self-healing system in blocking chloride penetration through the crack and the effectiveness of voltametric Ag sensors in detecting the presence of chlorides were investigated experimentally. High-performance cement mortar was chosen as the material to be studied, in order to ensure that optimal behaviour could be observed in non-cracked conditions.

1 Introduction

The sustainable development of societies can be pursued by simultaneously avoiding the depletion of materials and resources and reducing the greenhouse gases emissions, with related climatic change effects [1]. In order to get this, the extension of structures service-life plays a significant role in saving natural resources, decreasing the overall anthropogenic carbon-footprint, and reducing building and demolition wastes [1]. Indirectly the prolongation of the structures service-life reduces the energy consumptions and the heat emissions, which are among the main objectives of the Horizon 2030 program, since the construction industry is highly energy-intensive [2].

In order to achieve such prolongation of structures service-life [1], one of the most promising measures is the development of Smart Structures. These are defined as structures that are able to self-sense some external stimuli such as stress, wind-velocity or temperature variations, and internal conditions such as chloride penetration, concrete carbonatation, water availability, etc. They can also process the information and respond autonomously in real time by using smart materials technologies.

In the case of Reinforced Concrete Structures (RCS), the implementation of embedded sensors as part of a monitoring system, and the introduction of a self-healing technology, such as through the addition of

capsules, are promising solutions that can potentially turn ordinary RCS into Smart RCS [3,4].

Sensor systems configured by voltametric sensors have a great potential in the sense above specified [5,6]. In these sensors a potential sweep is applied, favouring the reaction of the different substances contained in the concrete pore solution with the sensor surface. Through the response signal it is possible to identify and quantify the presence of aggressive agents in the concrete pore solution, as well as to develop prediction models.

With this type of sensors, it is possible to create “Smart Multisensor Networks” (SMN), enhancing the discrimination and quantification power of the system. The SMN systems include models both initiation and propagation period, as defined in the Tutti, K. corrosion model [7]. In this way, the causes of durability loss can be determined early, reducing the energy and material resources employed to repair the deteriorated parts of the structures.

Deterioration and ageing of concrete are related to its porous network. But these are intensified when concrete is cracked. The presence of cracks modifies the concrete transport properties, creating favourable paths for fluids penetration; this can accelerate the chemical deterioration of RCS or the kinetics of steel corrosion [8], which is known to be one of the main causes of durability loss [9]. Important steps have been taken in the direction of concrete technology improvement in the last years,

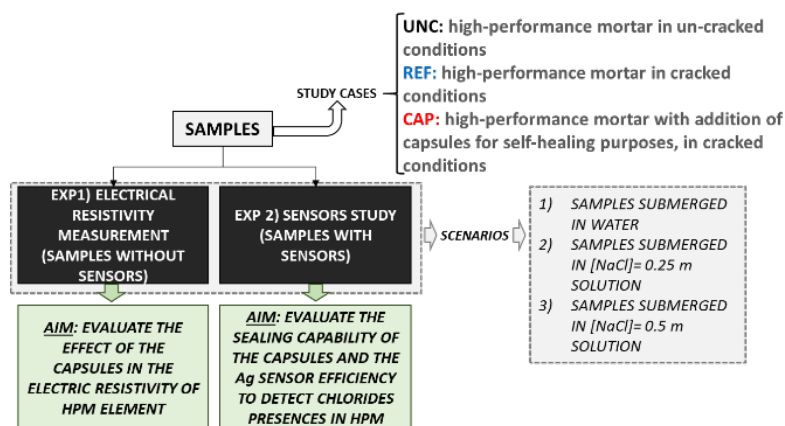


Fig. 1 Methodology scheme

which have enabled the design of concrete with extremely low porosity. However, cracks are still inevitable when concrete is in service.

In the case of high-performance concretes (HPC), it has been observed that the very low porosity of the matrix makes them even more brittle and sensitive to early age cracking than standard-concretes. This has resulted into the development of cracks-treating methodologies, which can be categorized into passive treatments that are applied manually after inspection and only heal the surface cracks, and active methods that are incorporated in the material, may fill both internal and external cracks, and are regarded as self-healing techniques [10,11].

In this report we propose a preliminary version of a smart structure system with self-healing and self-sensing properties, to demonstrate its effectiveness at a proof of concept level. The effectiveness of an active, capsule-based self-healing system in blocking the chlorides penetration through the crack and the effectiveness of voltametric Ag sensors in detecting the presence of chlorides were investigated experimentally. High Performance Mortar (HPM) was chosen as the material to be studied, in order to ensure that optimal behaviour could be observed in non-cracked conditions.

2 Materials and methods

2.1 Methodology

The aim of this experimental work consists in verifying the capability of the voltametric sensors to detect the penetration of Cl⁻ and the capability of the capsule-based system to seal the crack and block the penetration of chlorides. In this way the following cases were studied:

- UNC: high-performance mortar in un-cracked conditions
- REF: high-performance mortar in cracked conditions
- CAP: high-performance mortar with addition of capsules for self-healing purposes, in cracked conditions.

As described in Sections 2.4.1 and 2.4.2, cyclic voltammetry tests and electric resistivity tests were performed to characterize the behaviour of the proposed material.

The samples were conditioned over the following states in sequential steps for the purposes of performing the cyclic voltammetry tests:

- SAT: Saturated conditions. The samples were submerged in saturated Ca(OH)₂ solution in order to avoid the diffusion of pore solution hydroxide into the water where were the samples submerged. The samples were kept under this condition for 15 days.
- [NaCl]0.5m: Chloride exposure. The samples were submerged in [NaCl] 0.5 m solution during 66 days.

The overall experimental methodology followed is depicted in the scheme showed in Fig. 1.

2.2 Samples, sensors and capsules

The voltametric sensors were manufactured as depicted in Fig. 2-A, by using an Ag wire of 1 mm diameter. The average surface of the sensors was (0.27 ± 0.05) cm².

The self-healing capsules consisted of an epoxy-coated cementitious shell of cylindrical shape and a polyurethane precursor core (Fig. 2-B). Epoxy plaster was used to seal the capsules ends. The capsule composition details and manufacturing procedure were defined in accordance with Anglani G. et al. [12,13]. The polyurethane precursor (CARBOSTOP U, by API S.p.A., Italy) was selected based on its ability to react fast with ambient humidity, in such a way to create an expansive polyurethane foam for crack filling and sealing.

The sensors and capsules were embedded in prismatic samples of (4 x 4 x 16) cm³. Fig. 2-C shows the sensors and capsules locations within the sample.

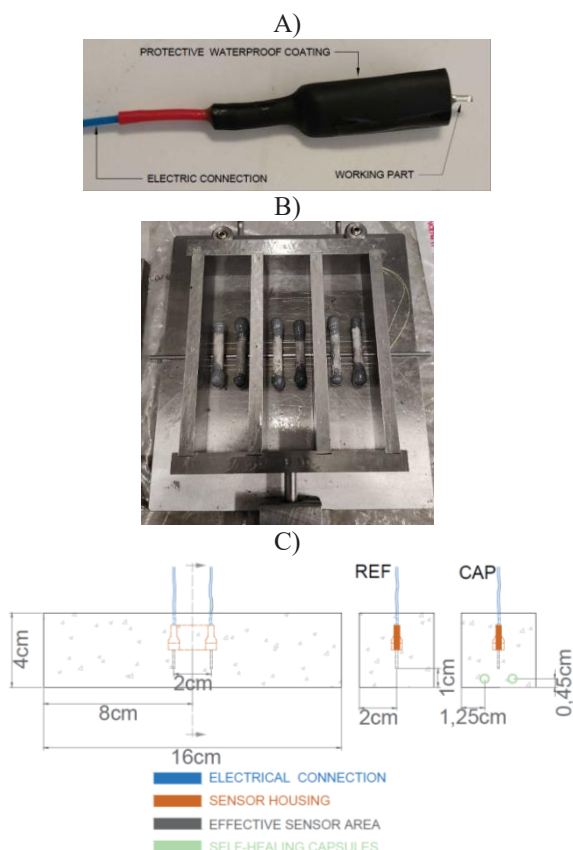


Fig. 2. A) Sensor. B) Capsules positioned in the mold. C) Sample scheme.

One sample was manufactured per each state (UNC, REF and CAP) with the sensor system embedded (ESS). Three samples per each state were manufactured in addition for the case without the sensor system embedded (NON-ESS). The total number of samples is then reported in Table 1.

Table 1 Number of samples

State	ESS	NON-ESS
UNC	1	3
REF	1	3
CAP	1	3
TOTAL	3	9

The mix design adopted for the HPM is detailed in Table 2.

Table 2. Composition of HPM

Materials	HPM (kg/m ³)
Ratio w/b*	0.32
Cement I 52.5 R (Buzzi Unicem)	500
Silica Fume (Mapeplast SF, by Mapei)	55
Water (tap water)	178
Natural Sand 0/4	1668
Superplasticizer (Dynamon SP1, by Mapei)	10

(*) Mass ratio between water and binder (i.e., cement plus silica fume).

To ensure a good material curing, the samples were stored for 28 days under a plastic foil in a humidity-saturated environment, at a temperature of (25 ± 2) °C.

2.3 Pre-cracking process and crack characterization

A localized crack was induced at mid span of the samples of the CAP and REF series by means of a three-point bending test performed with the aid of 25 kN closed-loop servo-controlled MTS hydraulic press (MTS 810, MTS Systems Corporation, USA).

Upon reaching the target value of 500 μm , the samples were unloaded at the same CMOD rate. The residual crack width upon unloading was measured via a stereomicroscope (SMZ18, Nikon Corporation, Japan), following the crack width measuring protocol described in Van Mullem et al. [14].

The average value of crack width was (248 ± 14) μm . Since all the specimens were pre-cracked following the same procedure, it was assumed that the average crack width was in the same range also for the samples of the CAP series, in which the crack mouth was hidden by the polyurethane foam.

2.4 Experimental techniques and tests

2.4.1 Sensor System. Electrochemical Techniques

CV (cyclic voltammetry) was applied with a 2-electrode configuration: the sensor acted as a working electrode and an external stainless steel sheet (96 cm²) was used as counter electrode/pseudo reference. This configuration was valid because the employed counter electrode had a much bigger surface than the working electrode [9]. Both techniques were applied by means of FRAPLUS potentiostat.

The CV was applied in the potentials range where the voltametric AgCl nucleation/formation take place [15]. The sweep rate was 20 mV/s.

2.4.2 Electric resistivity measurement

In order to obtain the electric resistivity of the samples, the direct method was applied according to the standard UNE 83988-1:2008, and the measure was taken with the conductivity meter Knick Portavo 902.

This conductivity meter was connected to two stainless steel sheets, which were placed in contact with the square bases the samples, as depicted Fig. 3. The electric connection with the concrete was ensured through a moist wipe.



Fig. 3. Set up for electrical conductance measurements.

The conductivity meter detected the electric conductance of the samples in the direction orthogonal to the metal sheets. The inverse of this value is the electric Resistance (R) in this direction. Through the relation established for a uniform electric field between two parallel rectangular sheet (equation 1), the electric resistivity ρ of the HPM in each state was then obtained [16].

$$\rho = R * \frac{S}{l} \quad (1)$$

S being the area of the cross-section and *l* length of the sample

2.4.3 Standard tests for the determination of the mechanical properties and the free chloride content

- Six additional plain mortar samples with the same mix-design (without capsules), casting procedure, and curing conditions were realized. They were used to preliminarily check the material flexural strength in three-point-bending in accordance with the standard UNI EN 196-1. After failure in bending, the residual portions of each sample (two halves) were tested in compression to assess the material compressive strength, always following the same standard, UNI EN 196-1. All these samples were tested at the age of 7 days.
- In the samples where the sensor system was embedded, the free chlorides quantity referred to the cement weigh was determined by the method explained in RILEM TC 178-TMC.

2.5 Sensor data analysis

The results obtained with the sensors system were analysed via the Principal Components Analysis (PCA) [17,18]. This analysis was performed based on the data matrix obtained through the CV results. This statistical tool allows to reduce the number of independent variables in a vector space of two dimensions, losing as less information as possible [17,18]. The axes of this new space are named Principal Components (PC). This representation makes the data interpretation easier. Therefore, in this study, the PCA allowed to identify the material state. This data processing protocol was applied by means of the toolbox for MATLAB [19].

3 Results

3.1 Standard tests for the determination of the mechanical properties and the free chloride content

Table 3 reports the results obtained in the standard tests for the determination of the material flexural strength and compressive strength. The flexural and compressive strength values achieved are in the typical range of HPM.

In addition, Table 4 shows the results obtained in the free chlorides test. They demonstrate that the polyurethane foam released from the capsules upon crack creation is able to seal the crack itself in such a way to produce the inhibition of chlorides penetration, reducing the %Cl_{cw} by a factor of two with respect to the ordinary crack conditions (REF).

Table 3 Mechanical properties of HPM

HPM batch	Flexural strength ^(°) (MPa)	Compressive strength ^(*) (MPa)
1	8.6 ± 0.7	100.3 ± 2.4
2	7.6 ± 0.3	87.3 ± 0.3

(°) Average value over three tests ± standard deviation
 (*) Average value over six tests ± standard deviation

Table 4 Percentage of free chlorides by weight of cement

	%Cl _{cw} (**)
UNC	0
REF	0.31
CAP	0.13

(**) Chlorides as a percentage by weight of cement

3.2 Analysis of the self-healing effect on the concrete electric resistivity

Fig. 4 shows the evolution over the time of the samples average electric resistivity for each concrete state (UNC, REF and CAP). It is possible to see how the samples with capsules have a bigger resistivity in the majority of the period than the other two series of samples. This is due to the fact that the polyurethane foam formed upon crack creation and interposed between the crack faces works as an electric insulation material. In this way the conductivity of the dielectric (HPM) is reduced, in other words the total dielectric constant is increased due to the healing agent sealing action on the crack.

In the case of the REF series (cracked condition), the crack width is relatively small, and the water and NaCl solution have a higher electric conductivity than the mortar matrix even in saturated conditions. Therefore, the crack does not seem to affect the electric resistivity much, compared with the UNC state.

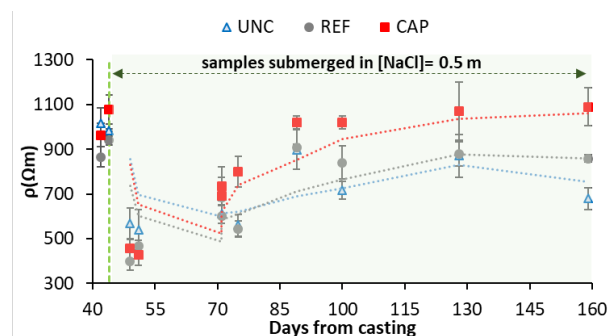


Fig. 4 Resistivity measures over time. Dash line shows moving average.

Considering this analysis, it can be concluded that the self-healing achieved through the addition of the

polyurethane-core capsules improves the behavior of the material against the coplanar macro-cell effect [20] even in comparison to the sound state (un-cracked conditions). We refer to coplanar macro-cell effect where the circulation of the ions takes place through the crack and in the direction orthogonal to the crack face (Fig. 5).

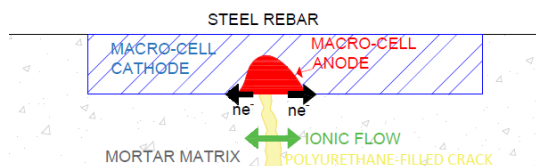


Fig. 5 Macrocell coplanar effect inhibition

3.2.1 Validation: colorimetric test

The titration of the free chlorides was conducted through a colorimetric method, consisting in spraying a solution of $AgNO_3$ all over the surfaces potentially interested by contact with chlorides. As it can be seen in the Fig. 6, the only surfaces where the chloride presence could be detected through this method were the surfaces belonging to the crack zone in the REF samples. The results obtained with the capsule-based self-healing system were promising because the results of this test point out the absence of free chlorides inside the crack, which indeed was almost perfectly sealed by the polyurethane foam released by the capsules. Therefore, the good behavior already manifested through the resistivity tests can be confirmed and it can be concluded that the crack-sealing effect produced by the encapsulated system is successful.

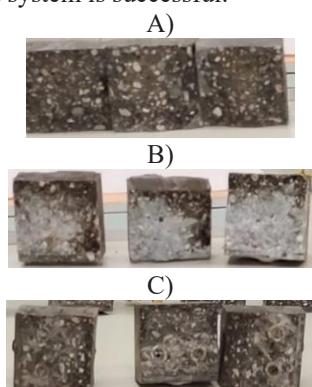


Fig. 6 Silver nitrate test pulverisation. A) UNC. B) REF. C) CAP

3.3 Effectiveness of the sensors and performance of the self-healing system in different states by means of PCA analysis.

Fig. 7 illustrates a graph of the PCA scores, and the distribution of specimens in the space formed by the first two PCs for all the states and conditions analysed. On the X-axis we find PC1, which accounts for 61.94 % of the variance in the data. PC2 appears on the Y-axis and explains 25.96 % of the variance in the data. The total of the variance in the data accounted for by the two axes is 87.9 %. Therefore, the PCA model represents well the information that was gathered through the

experiments. This is in good agreement with the scores indicated in other published studies [5,21,22].

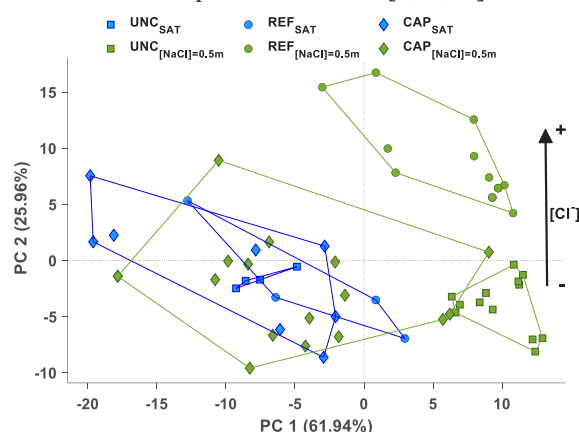


Fig. 7 PCA graph

In Fig. 7 we can see how the cluster of $REF_{[NaCl]=0.5m}$ are displaced with respect to the other clusters. Therefore, the sensor system is capable to identify the presence of chlorides when the concentration is of the order of 0.31 %_{vs.CW}, in agreement with the free chlorides standard test (Table 4).

When the concentration is of the order of 0.13 %_{vs.CW} or lower, the system is not capable to detect the chlorides presence, since the cluster of $CAP_{[NaCl]=0.5m}$ is virtually overlapped with the clusters related to SAT conditions.

4 Conclusions

This study reports the set-up and preliminary validation of a prototypal smart cement-based material with self-healing properties and an embedded voltametric sensor system for monitoring the chlorides penetration. According to the analysis performed, the following conclusions were depicted:

- The crack sealing achieved through the release of polyurethane foam from the capsule-based self-healing system produces an electric insulation enhancement from the point of view of coplanar macrocell effects and the inhibition of the chlorides penetration through the crack.
- The Ag voltametric sensor system is capable to identify the presence of chlorides starting from a minimum threshold of 0.31% of free chlorides referred to the cement weigh.

References

- [1] T.R. Naik, Sustainability of Concrete Construction, Pract. Period. Struct. Des. Constr. 13 (2008) 98–103. [https://doi.org/10.1061/\(ASCE\)1084-0680\(2008\)13:2\(98\)](https://doi.org/10.1061/(ASCE)1084-0680(2008)13:2(98)).
- [2] Global Energy Review 2020, OECD, 2020. <https://doi.org/10.1787/a60abbf2-en>.
- [3] G.S. Duffó, S.B. Farina, Development of an embeddable sensor to monitor the corrosion process of new and existing reinforced concrete structures, Constr. Build. Mater. 23 (2009) 2746–2751. <https://doi.org/10.1016/j.conbuildmat.2009.04.001>.
- [4] J.M. Gandía-Romero, R. Bataller, P. Monzón, I.

- Campos, E. García-Breijo, M. Valcuende, J. Soto, Characterization of embeddable potentiometric thick-film sensors for monitoring chloride penetration in concrete, *Sensors Actuators, B Chem.* **222** (2016) 407–418. <https://doi.org/10.1016/j.snb.2015.07.056>.
- [5] M. Alcañiz Fillol, Diseño de un sistema de lengua electrónica basado en técnicas electroquímicas voltamétricas y su aplicación en el ámbito agroalimentario, Universitat Politècnica de València, 2011. <https://doi.org/10.4995/Thesis/10251/11303>.
- [6] J.M. Gandía Romero, Sensores electroquímicos aplicados al estudio de la corrosión en estructuras de hormigón armado, Universitat Politècnica de València, 2014. <https://doi.org/10.4995/Thesis/10251/48516>.
- [7] K. Tutti, Corrosion of steel in concrete, Swedish Cement and Concrete Institute, Stockholm, 1982. <https://portal.research.lu.se/en/publications/corrosion-of-steel-in-concrete>.
- [8] C. Desmettre, J.P. Charron, Water permeability of reinforced concrete with and without fiber subjected to static and constant tensile loading, *Cem. Concr. Res.* **42** (2012) 945–952. <https://doi.org/10.1016/j.cemconres.2012.03.014>.
- [9] J.E. Ramón Zamora, Sistema de Sensores Embebidos para Monitorizar la Corrosión de Estructuras de Hormigón Armado. Fundamento, Metodología y Aplicaciones., Universitat Politècnica de València, 2018. <https://doi.org/10.4995/Thesis/10251/111823>.
- [10] N. De Belie, E. Gruyaert, A. Al-Tabbaa, P. Antonaci, C. Baera, D. Bajare, A. Darquennes, R. Davies, L. Ferrara, T. Jefferson, C. Litina, B. Miljevic, A. Otłowska, J. Ranogajec, M. Roig-Flores, K. Paine, P. Lukowski, P. Serna, J.M. Tulliani, S. Vucetic, J. Wang, H.M. Jonkers, A Review of Self-Healing Concrete for Damage Management of Structures, *Adv. Mater. Interfaces.* **5** (2018) 1–28. <https://doi.org/10.1002/admi.201800074>.
- [11] A. Negrini, M. Roig-Flores, E.J. Mezquida-Alcaraz, L. Ferrara, P. Serna, Effect of crack pattern on the self-healing capability in traditional, HPC and UHPFRC concretes measured by water and chloride permeability, *MATEC Web Conf.* **289** (2019) 01006. <https://doi.org/10.1051/mateconf/201928901006>.
- [12] G. Anglani, J.-M. Tulliani, P. Antonaci, Behaviour of Pre-Cracked Self-Healing Cementitious Materials under Static and Cyclic Loading, *Materials (Basel)*. **13** (2020) 1149. <https://doi.org/10.3390/ma13051149>.
- [13] G. Anglani, T. Van Mullem, J.-M. Tulliani, K. Van Tittelboom, N. De Belie, P. Antonaci, Durability of self-healing cementitious systems with encapsulated polyurethane evaluated with a new pre-standard test method, *Mater. Struct.* **55** (2022) 143. <https://doi.org/10.1617/s11527-021-01818-3>.
- [14] T. Van Mullem, G. Anglani, M. Dudek, H. Vanoutrive, G. Bumanis, C. Litina, A. Kwiecień, A. Al-Tabbaa, D. Bajare, T. Stryzewska, R. Caspeele, K. Van Tittelboom, T. Jean-Marc, E. Gruyaert, P. Antonaci, N. De Belie, Addressing the need for standardization of test methods for self-healing concrete: an inter-laboratory study on concrete with macrocapsules, *Sci. Technol. Adv. Mater.* **21** (2020) 661–682. <https://doi.org/10.1080/14686996.2020.1814117>.
- [15] Y. Guo, R.G. Compton, A bespoke chloride sensor for seawater: Simple and fast with a silver electrode, *Talanta.* **232** (2021) 122502. <https://doi.org/10.1016/j.talanta.2021.122502>.
- [16] P. Norberg, Electrical measurement of moisture content in porous building materials, *Durab. Build. Mater. Components.* **8** (1999) 1030–1039. <https://www.semanticscholar.org/paper/ELECTRICAL-MEASUREMENT-OF-MOISTURE-CONTENT-IN-Norberg/e6f29053e7d5d9b4ee09d3a929866bb7af0244a>.
- [17] F. Winquist, P. Wide, I. Lundström, An electronic tongue based on voltammetry, *Anal. Chim. Acta.* **357** (1997) 21–31. [https://doi.org/10.1016/S0003-2670\(97\)00498-4](https://doi.org/10.1016/S0003-2670(97)00498-4).
- [18] A. Martínez Ibernón, I. Gasch, J.M.G. Romero, J. Soto, Hardened Concrete State Determination System Based on a Stainless Steel Voltammetric Sensor and PCA Analysis, *IEEE Sens. J.* **22** (2022) 12947–12958. <https://doi.org/10.1109/JSEN.2022.3167612>.
- [19] D. Ballabio, A MATLAB toolbox for Principal Component Analysis and unsupervised exploration of data structure, *Chemom. Intell. Lab. Syst.* **149** (2015) 1–9. <https://doi.org/10.1016/j.chemolab.2015.10.003>.
- [20] P. Rodríguez, E. Ramírez, S. Feliu, J.A. González, W. López, Significance of Coplanar Macrocells to Corrosion in Concrete-Embedded Steel, *CORROSION.* **55** (1999) 319–325. <https://doi.org/10.5006/1.3283994>.
- [21] I. Campos Sánchez, Sensores electroquímicos tipo lengua electrónica voltamétrica aplicados al control medioambiental y a la industria alimentaria, Universitat Politècnica de València, 2013. <https://doi.org/10.4995/Thesis/10251/28937>.
- [22] H. Ji, W. Qin, Z. Yuan, F. Meng, Qualitative and Quantitative Recognition Method of Drug-producing Chemicals Based on SnO₂ Gas Sensor With Dynamic Measurement and PCA Weak Separation, *Sensors Actuators B Chem.* **348** (2021) 130698. <https://doi.org/10.1016/j.snb.2021.130698>.